Atomic Spectroscopy

Article

Study of the Change of Cr Speciation During the Diffusion-Reaction Process in Rock Samples Using Synchrotron Radiation Techniques

Hong Zhao,[a,b] Jiujiang Zhao,[a,*] Jing Zhang,[c] Caizhi Hu,[a] Yongbing Liu,[a] Wenbo Zhao,[a] and Zhaochu Hu [b]

[a] National Research Center for Geoanalysis, 26 Baiwanzhuang Street, Beijing 100037, P. R. China

[b] China University of Geosciences, Wuhan 430074, P. R. China

[c] Institute of High Energy Physics, Chinese Academy of Sciences, Beijing 100049, P. R. China

Received: *January 08, 2023;* ***Revised:*** *February 10, 2024;* ***Accepted:*** *February 20, 2024;* ***Available online:*** *February 20, 2024.*

DOI: 10.46770/AS.2024.001

ABSTRACT: To study the change of chromium speciation in the Cr(VI) natural attenuation processes, which involve both the diffusion and redox reaction of Cr(VI), Cr(VI) diffusion-reaction experiments for carbonate rock samples were conducted. The synchrotron radiation μ-XRF and SEM-EDS mapping revealed that in organic-rich carbonate rock samples, fresh precipitated Cr was mainly located near the surface and associated with organic matters. Whereas, in the sample with low organic matter, Cr was distributed evenly. These results indicate that the organic matter in the fractures and pore space is the major natural reductant that reacts with Cr(VI) in organic-rich samples, and forms reducing products (Cr(III) precipitates), which might aggregate and block the pore throats, and prevent further diffusion of Cr(VI) into the rock matrix. The synchrotron radiation X-ray absorption near-edge structure (XANES) was used to obtain the distributions of Cr chemical forms. The results show that for organic-rich samples, the $Cr(OH)_3$ fraction in the center was higher than that on the surface, whereas, for the samples containing low organic matter, no such significant difference was found. One possible explanation for these findings is that in organic-rich carbonate rock samples, the Cr(III) hydroxides, which aggregate in the zones near the surface, might age and transform from crystalline to the stable chemical forms of Cr(III) oxyhydroxide or even Cr(III) oxides, which could enhance the effect of Cr(VI) natural attenuation process. This work provides a feasible way to investigate the change of chromium chemical speciation during its diffusion-reaction processes in rock samples using synchrotron radiation techniques.

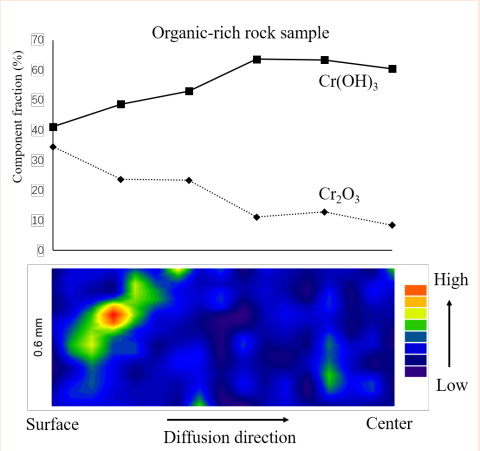

INTRODUCTION

Hexavalent chromium, Cr (VI), is toxic and carcinogenic,[1] which is a common contaminant released from anthropogenic activities in natural waters.[2] Cr (VI) is soluble in aqueous solution and exists in anionic forms (*e.g.* $HCrO_4^-$, CrO_4^- and $Cr_2O_7^{2-}$), which are strong oxidants and readily reduced to trivalent forms. Cr(III) is less toxic and soluble at low pH, whereas, as pH increases, it becomes insoluble precipitated as Cr(III)-hydroxide.[3,4] Several methods have been developed to remove Cr(VI) contamination, using physical and chemical techniques.[5,6] The traditional chemical reduction and precipitation processes are widely applied for Cr(VI) remediation using various reductants, such as zero-valent iron (Fe(0)), FeS and $FeSO_4$.[7–9] These processes could be low efficiency and generate secondary contamination.[5,6] In recent years, some relatively new approaches, which use nano-techniques and bioremediation have showed great potential for the remediation of Cr(VI) and been considered more effective, low cost and eco-friendly.[10,11]

The natural attenuation processes that work spontaneously in

natural environment,[12,13] are also considered for Cr(VI) remediation[14] with less cost and human intervention. Organic matters and Fe(II)-containing minerals are the major natural occurring reductants that react with Cr(VI) in natural attenuation processes. It is reported that natural organic matters (NOM) could reduce Cr(VI) in contaminated natural wetlands, and chromate resistant bacteria could remediate Cr(VI) via direct microbial reduction as well. Indirectly microbial reduction of Cr(VI) by dissimilar iron-reducing bacteria was also found in some zones of those wetlands.[15] The evidence for the natural attenuation of Cr(VI) in bedrock was reported in previous studies,[16,17] which reveals that Cr(VI) in porewater could be reduced by natural occurring reductants and form fresh Cr(III) precipitates in contaminated sandstone bedrock matrix.

When contaminants, such as Cr(VI), PCE or TCE, are released to the groundwater, they diffuse into the immobile porewater in bedrocks, resulting in the decrease of their concentrations in groundwater.[18,19] However, after cleaning process, the back diffusion of the contaminants from the rock matrix to the groundwater could prolong the remediation processes.[17,19,20] Therefore, the transport of Cr(VI) should also be considered for the Cr(VI) remediation. It is reported that the hydrodynamic conditions affected the migration of Cr(VI) and its natural attenuation process in unsaturated soil.[21] The diffusion of Cr(VI) is an important parameter for Cr(VI) groundwater contamination studies.[22] During the natural attenuation process, the chromium chemical forms changes, and the formation of Cr(III) precipitates might interfere with the Cr(VI) diffusion-reaction process.

To study chromium speciation, synchrotron radiation based X-ray absorption spectroscopy (XAS) techniques are widely used.[23,24] XAS, which includes X-ray absorption near edge structure (XANES) and extended X-ray absorption fine structure (EXAFS), can directly detect the oxidation states, chemical forms and structures for solid and liquid samples. In the study of Cr(VI) reduction within oil shales ashes, XANES and EXAFS were used for investigating the chromium chemical forms in different experimental conditions, and the results indicate that increasing pH is the controlling factor for Cr(VI) reduction process.[25] Combining micro-XANES mapping and scanning electron microscopy (SEM) analysis, the study on laboratory-simulated fire experiments showed that the stable species of Cr(III)-organic matter could be oxidized to Cr(VI) at high temperatures and become partly mobile, which increases the bioavailability and toxicity of chromium.[26]

To investigate the natural attenuation process of chromium, which involves the changes of chromium speciation, the diffusion of Cr(VI) into the carbonate rock samples and the interference of Cr(III) precipitates on the diffusion of Cr(VI) has been studied for understanding the mechanism of Cr(VI) diffusion-redox reaction in rock samples.

EXPERIMENTAL

Simulated natural attenuation experiments. Carbonate rock samples were obtained from Changxing, Zhejiang province, China. These rock samples were divided into two groups. The grey rock samples that contain low organic matter were selected as sample A, whereas the black and organic-rich rock samples were selected as sample B. Both sample A and B were cut as cubit blocks, which are approximately 2 × 2 × 2 cm. Sample blocks were soaked in the solution of 10g/L $K_2Cr_2O_7$ for about six weeks to ensure adequate diffusion and reaction; and other sample blocks were soaked in DI water for comparison. This method was modified from previous study on permanganate diffusion-reaction.[27] After the diffusion-reaction experiments, cross sections were cut in the middle of samples and polished thin sections were prepared for synchrotron radiation micro X-ray fluorescence (SR-μ-XRF), XANES, and SEM analysis.

To test the possible aging effect, fresh $Cr(OH)_3$ precipitates were made by soaking pyrite samples (1 × 1 × 1 cm) in the solution of 10g/L $K_2Cr_2O_7$, and the reducing products (fresh Cr(III) precipitates) were deposited on the surface of pyrite grains. Then these pyrite grains were washed and heated at 50°C. The aging time intervals were set as 14 and 35 days.

Synchrotron radiation XANES and μ-XRF analysis. Synchrotron radiation XANES and μ-XRF analyses were performed in Beijing Synchrotron Radiation Facility (BSRF), China. The Cr K-edge XANES spectra were measured at beamline 1W1B in BSRF with a storage ring of 2.5 GeV and 250 mA. The scans for the thin sections were collected in a fluorescence mode using a 19-element HPGe Detector from the surface of sample to the center with a step of about 2 mm, totally about 1 cm penetration depth. Linear combination fits (LCF) were performed on the normalized spectra using the IFEFFIT/Demter software package. XANES spectra were also measured for Cr reference materials including $K_2Cr_2O_7$, Cr_2O_3, and $Cr(OH)_3$, besides the samples for testing aging effect.

The SR-μ-XRF analysis was performed at 4W1B beamline in BSRF. The beam spot-size was focused down to ~ 50 μm and the μ-XRF raw data were processed by the standard procedures using the PyMca package.[28] The μ-XRF map scans were collected in the middle of the cross sections with a width of 0.6 mm.

X-ray diffraction（XRD）analysis. Powder X-ray diffraction analyses were conducted for rock samples with a Bruker D8 Discovery diffractometer. The X-ray source (Cu Ka) was operated at 40 kV and 40 mA with step scanning from 2θ values of 2–70°. The scanning step length was 0.02° with scanning time of 0.25s. The rock samples were crushed and passed through 325 mesh size (45 μm).

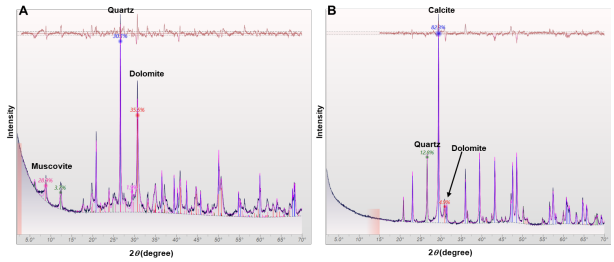

Fig. 1 Identification of various mineral phases in sample A and B under XRD.

Fig. 2 The BSE image and EDS maps of sample A and B after diffusion-reaction experiments. The direction of the diffusion is from the right side to the left side.

SEM-EDS analyses. Back scattered electron (BSE) images and elemental maps acquired with energy dispersive X-ray spectroscopy (EDS) were performed at National Research Center for Geoanalysis using a Zeiss Sigma 500 SEM equipped with a Bruker QUANTAX EDS system.

RESULTS AND DISCUSSION

Reaction sites in rock samples for Cr(VI). The XRD results (Fig. 1) indicate that the major minerals of sample A (with low organic matter) are dolomite, calcite, muscovite, whereas, those of rock sample B (organic rich) are calcite, and quartz.

To investigate the different Cr distribution patterns and identify the reaction sites for Cr(VI) in rock samples, scanning electron microscopy (SEM) was used. In a fractured porous rock system, in which water is confined within fractures, Cr(VI) can diffuse from fractures into porewaters driven by its concentration gradient, and then it can react with reducing minerals in the rock matrix.[19] As shown in SEM images (Fig. 2), Cr evenly distributed in rock sample A and no Cr deposition was found in the fractures. Some areas containing Cr were found to be associated with minerals containing sulfur and Fe(II), such as pyrite and chalcopyrite. Cr(VI) could be reduced by those reducing minerals forming Cr(III) precipitates, however, it is difficult to discriminate these precipitates from the natural Cr(III) minerals using EDS mapping. When Fe(II)-containing mineral is oxidized by Cr(VI), it transforms to Fe(III), ($Fe(OH)_3$), and then Cr(III) can substitute for Fe(III) forming mixed Cr(III)-Fe(III) hydroxides.[29] Those precipitates of Cr(III)-Fe(III) hydroxides have greater stability than Cr(III) hydroxides,[3] therefore Cr(III)-Fe(III) hydroxides could be the major forms of Cr(III) precipitates, when Fe(II)-containing minerals occurring. Fang et al. reported that during co-precipitated with $CaCO_3$, most Cr was adsorbed on the crystal surface of calcite or existed as amorphous Cr(III) hydroxide.[30] Therefore, the fresh Cr(III) precipitates could also be adsorbed by calcite in these rock samples.

Chromium distribution in rock samples. The SR-μ-XRF maps in Fig. 3 shows the distribution of Cr across the central line on the cross sections of the rock sample A and B after Cr(VI) reaction-diffusion experiments. Some naturally occurring Cr(III) minerals can be detected as well. Since the Cr(VI) can be adsorbed by some minerals, such as calcite.[30] In those samples, there was still a small amount of Cr(VI) that could be detected in both sample A and B, even after those samples were washed with DI water to remove soluble Cr(VI) before preparing thin sections. When Cr(VI) diffused into these rock samples, it reacted with natural reductants and was reduced to Cr(III) precipitates, which deposited at the reaction sites. A variety of natural reductants can react with Cr(VI), including Fe(II) containing minerals, sulfur and organic carbon [12]. In sample A, the Cr content distributed evenly from surface to the center, which indicates that Cr(VI) can diffuse through the whole sample during the experiment and might fill the fractures and pores of this sample. In sample B, the high Cr spots were only found close to the surface, whereas the Cr content was relatively low in the center. This indicates that Cr(VI) cannot penetrate into the center of sample B even after 6 weeks.

EDS maps (Fig. 2B) show that Cr was obviously deposited in the fractures in sample B, and most of Cr distributed close to the fractures. Some areas containing high Cr content were visibly associated with organic matters, which is the evidence that organic

Fig. 3 SR-μ-XRF maps of the distribution of Cr across the central line on the cross sections of sample A and B after diffusion-reaction experiments. Cr(VI) diffuses from both left and right sides of sample A and B. The lengths of the figures have been adjusted and do not reflect the real length-width ratio.

Fig. 4 Normalized XANES spectra for samples after Cr(VI) diffusion-reaction experiment a: sample A and B after reaction with Cr(VI), and sample B soaked in DI water (no reaction); b: the Cr(III) precipitate sample (pyrite) ages for 14 and 35 days at 50°C. And the spectra for chromium standards Cr(VI), Cr_2O_3, and $Cr(OH)_3$.

matters react with Cr(VI). Cr content is relatively higher on the right side than on the left side, which follows the Cr(VI) diffusion direction in sample B. When Cr(VI) diffuses into an organic-rich rock sample, in which organic matters occur in the fractures and pores, it reacts with these organic matters first forming Cr(III) precipitates, which can be deposited on the surface of fractures and pores. As Cr(III) precipitates increase, they possibly aggregates and blocks the pore throat. The accumulation of Cr(III) precipitates retards the diffusion of Cr(VI), which prevents Cr(VI) from further penetrating into the center of the rock sample (Fig. 3B). On the contrary, when Cr(VI) diffuses into the rock sample with low organic content, it can pass through the fractures and diffuse into the pores, without redox reaction, therefore Cr(VI) can contact the natural occurring reducing minerals in the rock matrix and be reduced and deposited associated with those minerals, as shown in Fig. 3A. Similar to Cr(VI), permanganate (Mn(VII)) have been found that can also be reduced by natural reductants and form MnO_2 precipitates[27] and block the pore throats and even fill the whole pore space,[31] when Mn (VII) is used as an oxidant for *in-situ* chemical oxidation (ISCO) of groundwater contaminants, such as PCE and TCE.[13,32,33]

The changes of chromium chemical forms during the diffusion-reaction processes. To investigate the chemical form changes of chromium during the experiments, the XANES spectra for rock samples were measured. Fig. 4(a) displays the normalized XANES spectra for the sample A and B after diffusion-reaction experiments, and the sample B that was soaked in DI water (no reaction). The chromium standards, including Cr(VI), Cr_2O_3, and $Cr(OH)_3$, were also determined. Cr(VI) can be identified by its distinct pre-edge peak (~5993 eV) in XANES spectra, whereas, the differences in near-edge structures can be used to distinguish the different chemical forms of Cr(III).[34,35] Comparing amorphous $Cr(OH)_3$, the spectra of the crystalline Cr_2O_3 shows more complex structures.[4]

The Cr content in the Cr distribution maps (Figs. 2 and 3) could be Cr(III) precipitates, which is the reducing products of Cr(VI). The component fractions of different chromium forms were obtained by linear combination fitting for their normalized XANES spectra. The profiles (Fig. 5) show that the percentage distribution of chromium chemical forms from the surface to the center of these samples. For sample A, no significant changes in chromium chemical forms were found. The Cr_2O_3 fractions can be considered as background Cr in rock samples, which occurs as natural Cr(III) minerals. The fractions of $Cr(OH)_3$ is the reducing products of Cr(VI), which penetrates into rock matrix and is reduced by natural occurring reductants, such as Fe(II)-containing minerals. For sample B, the percentage fraction of $Cr(OH)_3$ increased with the penetration distance of Cr(VI), whereas, that of Cr_2O_3 decreased. The Cr_2O_3 found in sample B could be from the impurity of natural Cr(III) minerals in these rock samples, such as chromite, olivine and pyroxene.[17]

Another explanation for these findings could be the aging effect of $Cr(OH)_3$. The fresh Cr(III) precipitates deposited in the pore space and could block the pore throats, therefore the diffusion flux of Cr(VI) became low, which increased the Cr(VI) concentration close to the surface of sample B, and allowed more Cr(VI) to react with organic matters and form more precipitates. Those Cr(III) precipitates could aggregate and transform crystalline $Cr(OH)_3$ structure into stable amorphous $Cr(OH)_3$ [36] during the experiments. It is reported that after aging, $Cr(OH)_3$ could form oxyhydroxide, $CrO_{(3-x)/2}(OH)_x$, and eventually transform to chromium(III) oxide, Cr_2O_3, after heating and aging.[37,38] Compared to Cr(III) hydroxides, Cr_2O_3 is a more stable chemical form of chromium. The chemical form changes might lead to more Cr_2O_3-like XANES spectra for

Fig. 5 The percentage distribution of chromium chemical forms, which were obtained via linear component fitting, at different penetration depths of Cr(VI) in sample A and B. XANES spectra were collected about every 2 mm. ◆ represents Cr_2O_3; ■ represents $Cr(OH)_3$; ▲ represents Cr(VI).

the Cr(III) precipitates, which can be found from data fitting. Only a small amount of Cr(VI) penetrated into the center of sample B, and if it was reduced by natural reductants, the fresh reducing product of $Cr(OH)_3$ might retain its chemical forms, resulting in greater $Cr(OH)_3$ fraction in the center than that on the surface.

The XANES spectra of the samples for testing the possible aging effect are shown in Fig. 4(b). The LCF data fitting results show that with the increasing of aging time from 14 days to 35 days, the percentage fractions of $Cr(OH)_3$ decreased from 65% to 52%, whereas that of Cr_2O_3 fractions increased from 11% to 21%, which proves that aging effect of $Cr(OH)_3$ during natural attenuation processes could transform $Cr(OH)_3$ to more stable chemical forms, such as Cr_2O_3. It should be noted that the aging experiment was done at the temperature of 50°C, which may not reflect the real situation in natural attenuation processes. As reported, the solubility of amorphous $Cr(OH)_3$ is below the 50 µg/l (EU drinking water limit) at the pH range of 5.7 to 11, which can be considered as safe.[36] Those chemical forms are more inert and might prevent Cr(III) from being oxidized to Cr(VI) and then returning to porewaters, which ensures the natural attenuation process long-term effective. Previous study reported that the fresh Cr(III) precipitates formed in Cr(VI) contaminated bed rock could be extracted by hydrogen peroxide, indicating that these precipitates are unstable in oxidation environment and can be remobilized in presence of natural oxidants [17].The aging effect might change the chemical forms of Cr(III) precipitate and increase its stability, which enhances the effect of natural attenuation of Cr(VI).

CONCLUSION

This study reveals that the natural attenuation process for Cr(VI) remediation is affected by both diffusion and redox reaction of chromium. The formation of Cr(III) precipitates during natural attenuation process could interfere with the diffusion of Cr(VI) into the bedrock matrix. When Cr(VI) diffuses into the rock samples, it reacts with natural occurring reductants in the rock matrix forming Cr(III) hydroxide. The results show that in Cr(VI) natural attenuation processes, Cr(III)-precipitates might aggregate and block the pore throats or even the fractures, which prevent the diffusion of Cr(VI) into the rock matrix and decrease the efficiency of natural attenuation for Cr(VI). The evidence for this effect has been found in organic-rich rock samples, in which the organic matters extensively and evenly distribute in fractures and pores. Whereas, for the sample that contains low organic matter, no such evidence has been found, and Cr(VI) can diffuse through the fractures or pores into the rock matrix without being reduced to Cr(III). The aging effect might transform Cr(III)-precipitates to more stable chemical forms similar to chromium oxides, which could improve the efficacy of the natural attenuation process for Cr(VI). This work provides a way to study chromium speciation during its diffusion-reaction processes in rock samples using synchrotron radiation techniques. Further studies are needed to prove the hypothesis for aging effect and reveal the diffusion-reaction mechanism of Cr(VI) natural attenuation process, using *in-situ* micro analysis techniques.

AUTHOR INFORMATION

Jiu-Jiang Zhao received his BSc in 1999 from Peking University, and PhD in 2009 from Carleton University, Canada. He is a research scientist in National Research Center for Geoanalysis, Chinese Academy of Geological Sciences. His major research interests are environmental chemistry, analytical chemistry, chemical speciation and bioavailability, and the applications of diffusive gradients in thin-film techniques and the synchrotron radiation techniques. Jiu-Jiang Zhao is author or co-author of over 30 articles published in peer-reviewed scientific journals.

Corresponding Author

* J. J. Zhao

Email address: zhao_jiujiang@hotmail.com

Notes

The authors declare no competing financial interest.

ACKNOWLEDGMENTS

The authors gratefully acknowledge the financial support from the National Natural Science Foundation of China (U1932113 and 21605030) and the National Key Research and Development Project of China (2019YFC1805001). The staff members of beamline 1W1B and 4W1B of Beijing Synchrotron Radiation Facility, Institute of High Energy Physics, Chinese Academy of Sciences are acknowledged for their support in measurements of XANES and μ-XRF.

REFERENCES

1. V. Gómez and M. P. Callao, *TrAC - Trends Anal. Chem.*, 2006, **25**, 1006–1015. https://doi.org/10.1016/j.trac.2006.06.010
2. M. Shahid, S. Shamshad, M. Rafiq, S. Khalid, I. Bibi, N. K. Niazi, C. Dumat, and M. I. Rashid, *Chemosphere*, 2017, **178**, 513–533. https://doi.org/10.1016/j.chemosphere.2017.03.074
3. B. M. Sass and D. Rai, *Inorg. Chem.*, 1987, **26**, 2228–2232. https://doi.org/10.1021/ic00261a013
4. D. Rai, D. a. Moore, N. J. Hess, K. M. Rosso, L. Rao, and S. M. Heald, *J. Solution Chem.*, 2007, **36**, 1261–1285. https://doi.org/10.1007/s10953-007-9179-5
5. S. Guo, C. Xiao, N. Zhou, and R. Chi, *Environ. Chem. Lett.*, 2021, **19**, 1413–1431. https://doi.org/10.1007/s10311-020-01114-6
6. M. Krishna, P. Khandayataray, and D. Samal, *J. Environ. Manage.*, 2022, **318**, 115620. https://doi.org/10.1016/j.jenvman.2022.115620
7. X. Lv, J. Xu, G. Jiang, J. Tang, and X. Xu, *J. Colloid Interface Sci.*, 2012, **369**, 460–469. https://doi.org/10.1016/j.jcis.2011.11.049
8. H. Lyu, J. Tang, Y. Huang, L. Gai, E. Y. Zeng, K. Liber, and Y. Gong, *Chem. Eng. J.*, 2017, **322**, 516–524. https://doi.org/10.1016/j.cej.2017.04.058
9. Q. A. Nguyen, B. Kim, H. Y. Chung, A. Q. K. Nguyen, J. Kim, and K. Kim, *Ecotoxicol. Environ. Saf.*, 2021, **208**, 111735. https://doi.org/10.1016/j.ecoenv.2020.111735
10. S. Younan, G. Z. Sakita, T. R. Albuquerque, R. Keller, and H. Bremer-Neto, *J. Sci. Food Agric.*, 2016, **96**, 3977–3982. https://doi.org/10.1002/jsfa.7725
11. Z. Chen, D. Wei, Q. Li, X. Wang, S. Yu, L. Liu, B. Liu, S. Xie, J. Wang, D. Chen, T. Hayat and X. Wang, *J. Clean. Prod.*, 2018, **181**, 745–752. https://doi.org/10.1016/j.jclepro.2018.01.231
12. C. D. Palmer and R. W. PuIs, *EPA Ground Water Issue: Natural Attenuation of Hexavalent Chromium in Groundwater and Soils*, 1994.
13. N. A. Khan and K. C. Carroll, *Chemosphere*, 2020, **247**, 125848. https://doi.org/10.1016/j.chemosphere.2020.125848
14. USEPA, *Superfund remedy report. 16th edition. United States Environmental Protection Agency, Arlington, VA.* https://www.epa.gov/remedytech/superfund-remedy-report, 2020.
15. K. Jiang, J. Zhang, Z. Deng, S. Barnie, J. Chang, Y. Zou, X. Guan, F. Liu, and H. Chen, *Environ. Pollut.*, 2021, **287**, 117639. https://doi.org/10.1016/j.envpol.2021.117639
16. J. Zhao, T. Al, S. W. Chapman, B. Parker, K. R. Mishkin, D. Cutt, and R. T. Wilkin, *Chem. Geol.*, 2015, **419**, 142–148. https://doi.org/10.1016/j.chemgeo.2015.10.034
17. J. Zhao, T. Al, S. W. Chapman, B. L. Parker, K. R. Mishkin, D. Cutt, and R. T. Wilkin, *Chem. Geol.*, 2017, **474**, 1–8. https://doi.org/10.1016/j.chemgeo.2017.10.004
18. S. Chapman, B. Parker, T. Al, R. Wilkin, D. Cutt, K. Mishkin, and S. Nelson, EPA/Science Inventory, 2021, 408–413. https://doi.org/10.3390/soilsystems5010018
19. B. L. Parker, S. W. Chapman, and J. A. Cherry, *Ground Water*, 2010, **48,** 799–808. https://doi.org/10.1111/j.1745-6584.2010.00755.x
20. R. C. Borden and K. Y. Cha, *J. Contam. Hydrol.*, 2021, **243**, 103889. https://doi.org/10.1016/j.jconhyd.2021.103889
21. Y. Wei, X. Xu, L. Zhao, X. Chen, H. Qiu, B. Gao, and X. Cao, *J. Hazard. Mater.*, 2021, **416**, 126229. https://doi.org/10.1016/j.jhazmat.2021.126229
22. A. K. Tiwari, S. Orioli, and M. De Maio, *J. Contam. Hydrol.*, 2019, **225**, 103503. https://doi.org/10.1016/j.jconhyd.2019.103503
23. H. L. Huang and Y. J. Wei, *Chemosphere*, 2018, **194**, 390–395. https://doi.org/10.1016/j.chemosphere.2017.11.160
24. Y. V. Nancharaiah, C. Dodge, V. P. Venugopalan, S. V. Narasimhan, and A. J. Francis, *Appl. Environ. Microbiol.*, 2010, **76**, 2433–2438. https://doi.org/10.1128/AEM.02792-09
25. T. El-Hasan, W. Szczerba, G. Buzanich, M. Radtke, H. Riesemeier, and M. Kersten, *Environ. Sci. Technol.*, 2011, **45**, 9799–9805. https://doi.org/10.1021/es200695e
26. I. Rascio, I. Allegretta, C. E. Gattullo, C. Porfido, G. P. Suranna, R. Grisorio, K. M. Spiers, G. Falkenberg, and R. Terzano, *J. Hazard. Mater.*, 2022, **436**, 129117. https://doi.org/10.1016/j.jhazmat.2022.129117
27. Q. Huang, H. Dong, R. M. Towne, T. B. Fischer, and C. E. Schaefer, *J. Contam. Hydrol.*, 2014, **159**, 36–46. https://doi.org/10.1016/j.jconhyd.2014.01.010
28. V. A. Solé, E. Papillon, M. Cotte, P. Walter and J. Susini, *Spectrochim. Acta B*, 2007, **62**, 63–68. https://doi.org/10.1016/j.sab.2006.12.002
29. Y. Tang, F. M. Michel, L. Zhang, R. Harrington, J. B. Parise, and R. J. Reeder, *Chem. Mater.*, 2010, **22**, 3589–3598. https://doi.org/10.1021/cm1000472
30. Z. Fang, W. Liu, T. Yao, G. Zhou, S. Wei, and L. Qin, *Geochim. Cosmochim. Acta*, 2022, **322**, 94–108. https://doi.org/10.1016/j.gca.2022.01.019
31. M. A. Urynowicz, B. Balu, and U. Udayasankar, *J. Contam. Hydrol.*, 2008, **96**, 187–194. https://doi.org/10.1016/j.jconhyd.2007.11.001
32. K. Y. Cha, M. Crimi, M. a. Urynowicz, and R. C. Borden, *Environ. Eng. Sci.*, 2012, **29**, 646–653. https://doi.org/10.1089/ees.2011.0211
33. X. Xu and N. R. Thomson, *J. Environ. Eng.*, 2008, **134**, 353–361. https://doi.org/10.1061/(ASCE)0733-9372(2008)134:5(353)

34. Z. Fang, L. Qin, W. Liu, T. Yao, X. Chen, and S. Wei, *Natl. Sci. Rev.*, 2021, **8**, 151–158. https://doi.org/10.1093/nsr/nwaa090

35. A. U. Rajapaksha, M. S. Alam, N. Chen, D. S. Alessi, A. D. Igalavithana, D. C. W. Tsang, and Y. S. Ok, *Sci. Total Environ.*, 2018, **625**, 1567–1573. https://doi.org/10.1016/j.scitotenv.2017.12.195

36. N. Papassiopi, K. Vaxevanidou, C. Christou, E. Karagianni, and G. S. E. Antipas, *J. Hazard. Mater.*, 2014, **264**, 490–497. https://doi.org/10.1016/j.jhazmat.2013.09.058

37. N. Torapava, A. Radkevich, D. Davydov, A. Titov, and L. Persson, *Inorg. Chem.*, 2009, **48**, 10383–10388. https://doi.org/10.1021/ic901539g

38. V. Swayambunathan, Y. X. Liao, and D. Meisel, *Langmuir*, 1989, **5**, 1423–1427. https://doi.org/10.1021/la00090a030